

---

# Relationship between Crumb Rubber Morphology and Asphalt Rubber Viscosity

**Ezio Santagata\*** — **Davide Dalmazzo\*** — **Michele Lanotte\***  
**Maria Chiara Zanetti\*** — **Barbara Ruffino\***

*\* Politecnico di Torino*

*Department of Environmental, Land and Infrastructure Engineering*

*24, corso Duca degli Abruzzi*

*10129 Torino, Italy*

*ezio.santagata@polito.it*

*davide.dalmazzo@polito.it*

*michele.lanotte@polito.it*

*mariachiara.zanetti@polito.it*

*barbara.ruffino@polito.it*

---

*ABSTRACT. The experimental investigation described in this paper refers to the assessment of the relationship between morphology of crumb rubber particles and viscosity of corresponding asphalt rubber binders. Analyses were carried out on crumb rubber products derived from ambient, cryogenic and high pressure waterjet size-reduction processes. Asphalt rubber binders were prepared with a common base bitumen and crumb rubber dosage. An innovative technique based on the combined use of microscopic observations, image analysis algorithms and three-dimensional particle models was developed for the quantitative evaluation of the morphological characteristics of crumb rubber. Viscosity tests were carried out on binders in a wide temperature range at a given shear rate. Results of morphological analyses were coherent with each other and totally compatible with the information regarding production processes. A clear viscosity ranking of asphalt rubber binders was established, highlighting the peculiarities of different types of crumb rubber. A prediction model was proposed which shows the dependency of viscosity on the morphological characteristics of crumb rubber. The model proved to be statistically sound and in agreement with the interaction phenomena which occur within asphalt rubber binders.*

*KEYWORDS: asphalt rubber, morphology, surface area, rheology, viscosity.*

---

## 1. Introduction

Asphalt rubber binders for paving applications are prepared by combining bitumen with crumb rubber (CR) derived from end-of-life tyres (ELTs) in specialized production plants. Knowledge on their physical and rheological properties has significantly evolved since their initial conception in the early sixties, with the consequent identification of a number of issues which have to be taken into account in the selection of component materials, in the production of the composite binders and in their end-use as part of high-performance bituminous mixtures (Hicks, 2002; State of California Department of Transportation, 2005).

Even though a massive amount of research on asphalt rubber binders has been carried out worldwide, the mechanisms of interaction between bitumen and CR are not fully understood. In particular, with respect to the flow behaviour of the binders, effects due to variations in the physical and morphological characteristics of CR still need to be clearly identified. Contributions in this area of research are therefore necessary in order to optimize production operations with the consequent preparation of high-performance binders.

Research studies on the morphology of CR particles have highlighted the difference between “ambient” and “cryogenic” products, respectively deriving from mechanical milling operations at ambient temperature and from impact-type fragmentation at low temperature. By means of microscopic observations it has been established that CRs of the first type generally exhibit irregular shape and rough surface, while those of the second type are of a more cuboid-type morphology with sharper edges and smoother surfaces (West *et al.*, 1998; Shen *et al.*, 2005; Lee *et al.*, 2008; Thodesen *et al.*, 2009). However, such information has not been expressed in quantitative terms and has not been used as an input to any model for the prediction of the rheological properties of corresponding asphalt rubber binders.

Several physical properties of CRs have been considered within experimental investigations performed on asphalt rubber binders. These include both the ones which are mentioned in ASTM standard D6114 (maximum particle size and specific gravity) and those which are taken into account in technical specifications (e.g. size distribution). Considerable efforts have been spent in the evaluation of surface area (referred to the unit mass or unit volume) which is believed to closely control the interaction of CR with bitumen during mixing and curing operations. This has been done by employing low-temperature gas sorption techniques and the Brunauer, Emmett and Teller (BET) method (West *et al.*, 1998; Shen *et al.*, 2009a,b) which however may lead to an overestimate of surface area depending upon specific rubber properties. In any case, it has been observed that due to the different particle morphology and surface porosity, cryogenic CRs have a higher density and a lower surface area than ambient CRs.

Viscosity measurements performed on asphalt rubber binders containing different types and dosages of CR have been included in many experimental investigations documented in literature. This is due to the fact that viscosity is considered as an excellent binder quality indicator, sensitive to the time-dependant interaction effects which occur between the two components and directly related to the rheological behaviour which the binders exhibit in the field under the effects of traffic and environmental loading.

A number of studies have focused on the influence on binder viscosity of particle size and surface area (Putman *et al.*, 2006; Shen *et al.*, 2009a,b; Thodesen *et al.*, 2009). In such a context, it has been observed that as surface area increases, as a result of the absorption of lighter bitumen fractions, viscosity tends to increase. However, such an effect can be counterbalanced by the fact that surface area decreases with the increase of particle size which in turn leads to higher viscosity values (Shen *et al.*, 2009a).

According to experimental evidence, the flow behaviour of binders is also sensitive to CR type, dosage and composition. In particular, due to differences in their morphology and composition, cryogenic CRs have been found to be less effective than ambient CRs in increasing the viscosity of asphalt rubber binders (West *et al.*, 1998). Moreover, it has been pointed out that such products may require a greater mixing and curing time as a result of the lower reaction rate which controls their interaction with bitumen (Shen *et al.*, 2005). For CRs of both types, a number of investigations have confirmed that the rheological properties of resulting binders is strongly dependent upon their composition and on that of base bitumen.

The issues synthesized above have been taken into consideration by the authors as part of their ongoing effort in giving scientific support to the implementation of asphalt rubber related technologies (Zanetti *et al.*, 2011; Santagata *et al.*, 2012). In particular, the results which are reported in this paper refer to an experimental investigation the purposes of which were on one hand to develop innovative techniques and models for the assessment of the morphological characteristics of CRs, and on the other hand to identify their possible quantitative relationship with the flow properties of asphalt rubber binders. Tests were carried out on CRs deriving from ambient, cryogenic and high pressure waterjet production processes, combined with a single reference bitumen. Results were quite encouraging and will form the basis for the future enhancement of the characterization methods and of the proposed viscosity prediction model.

## 2. Materials

### 2.1. Crumb rubber

CR samples were taken from five ELT processing plants where size-reduction operations are combined with other treatments (e.g. shredding, iron separation, granulation and sieving) in configurations which depend upon available technologies, inflow of material and desired quality of end products (Table 1).

Three of the considered plants (A, B and C) operate the so-called “ambient size reduction” by means of four consecutive processing phases consisting in shredding, iron magnetic separation, milling and sieving. However, in the case of plant B, shredding is carried out in two steps, with an extra phase of iron separation, and with an additional intermediate cold granulation treatment. This should lead to the production of CR characterized by a high degree of purity and constituted by more cubical and uniformly shaped particles.

Plant G operates in cryogenic conditions by making use of liquid nitrogen, which cools rubber granules down to  $-80^{\circ}\text{C}$  under an inert atmosphere, and by employing high impact hammer mills. It is thus claimed that the resulting particles are of a cuboid-type morphology with smooth surfaces and small porosity. Moreover, as a result of the specific treatment conditions, molecular chains of rubber polymers are presumably not degraded and elastic properties are consequently fully preserved.

Plant H is a reduced-scale pilot plant which has been designed to implement the innovative High Pressure WaterJet technology. It is based on the use of high pressure (approximately 3.000 bar) water jets which may generate CR characterized by a high degree of purity.

According to owners, all the considered plants employ both car and truck tyres. The only exception is constituted by plant C, which collects exclusively ELTs coming from heavy vehicles, characterized by a higher natural rubber content.

**Table 1.** Configuration of ELT processing plants

	A	B	C	G	H
Primary shredding	×	×	×	×*	n.a.
Iron magnetic separation		×			n.a.
Secondary shredding		×			n.a.
Cold granulation		×			n.a.
Iron magnetic separation	×	×	×	×	n.a.
Milling	×	×	×	×*	× <sup>o</sup>
Sieving	×	×	×	×	

(\*) Carried out in cryogenic conditions.

(<sup>o</sup>) Substituted by waterjet blasting.

n.a. Not applicable.

## 2.2. Asphalt rubber

In order to compare their effectiveness as modifiers in the production of asphalt rubber binders, the different CRs were combined with the same 50/70 penetration base bitumen with a constant dosage of 15% by weight of the total binder. Mixing was carried out by operating on 500 g batches by means of a mechanical mixer, equipped with an anchor-shaped stirrer, by imposing a rotation speed of 600-700 rpm for 90 minutes. During production operations temperature was maintained at  $180 \pm 5^\circ\text{C}$  by means of a thermostatic oil bath. The mixing protocol was adopted for all asphalt rubber binders regardless of specific reaction rates of employed CRs.

## 3. Methods

### 3.1. Morphology and surface area of crumb rubber particles

CR samples taken from the processing plants were subjected to laboratory tests for the determination of particle size distribution and density. Moreover, by means of the combined use of microscopic observations, image analysis algorithms and three-dimensional analytical models, they were characterized in terms of particle morphology and surface area.

Particle size distribution analysis was performed in dry conditions by making use of sieves of the Tyler series. Density ( $\rho$ ) at  $25^\circ\text{C}$  was evaluated with the pycnometer method by employing ethylic alcohol as the fluid of known density in order to prevent particles from floating to the surface. Relative density (i.e. specific gravity, SG) was calculated by referring measured density to that of water at the same temperature.

Assessment of the morphological characteristics of CR particles was carried out by employing a stereomicroscope equipped with a digital camera and by processing the resulting images with a freeware software (ImageJ, version 1.45, National Institutes of Health). However, in the case of CR H it was found that due to the very high content of fine particles (passing the 0.063 mm sieve) it was necessary to perform the analyses on single-size fractions obtained by employing the same sieve series used for size distribution evaluation.

For each CR (or CR fraction) the following parameters were derived from the plan-view image of the set of considered particles:

- average value of the shape coefficient ( $C_f$ ), given by the ratio between the maximum and minimum Feret diameters (maxF and minF) of the particle (Figure 1);
- average value of the solidity coefficient ( $C_s$ ), given by the ratio between the area of the particle ( $A_{\text{particle}}$ ) and the minimum convex area ( $A_{\text{convex}}$ ) in which it is enclosed (Figure 1);
- shape ( $\phi_f$ ) and roughness ( $\phi_r$ ) factors, employed to estimate surface area per unit mass ( $SA_m$ ) by means of the following expression:

$$SA_m = w \cdot \frac{6}{\dots} \cdot \sum_i \frac{f_i}{d_{m,i}} \quad [1]$$

where:  $SA_m$  = surface area per unit mass (in  $m^2/g$ );  
 $\phi$  = corrective factor, given by the product of the shape ( $\phi_f$ ) and roughness ( $\phi_r$ ) factors ( $\phi = \phi_f \cdot \phi_r$ );  
 $\rho$  = density (in  $g/m^3$ );  
 $f_i$  = frequency (in decimal units) of the  $i$ -th single-size fraction;  
 $d_{m,i}$  = mean particle diameter (in m) of the  $i$ -th fraction.

The abovementioned shape and roughness factors ( $\phi_f$  and  $\phi_r$ ) were calculated by modeling each CR particle (Figure 2):

- as a sphere with a diameter ( $d_s$ ) equal to the minimum Feret diameter (“S” model);
- as an ellipsoid (prolate spheroid) with an area of the maximum cross-section ( $A_{\text{ellipse}}$ ) equal to the area of the projection of the particle on the horizontal plane ( $A_{\text{particle}}$ ) (“E” model);
- as an ellipsoid (prolate spheroid) with area and perimeter of the maximum cross-section ( $A_{\text{ellipse}}$  and  $P_{\text{ellipse}}$ ) equal to the area and perimeter of the projection of the particle on the horizontal plane ( $A_{\text{particle}}$  and  $P_{\text{particle}}$ ) (“R” model, which takes into account particle surface roughness).

By considering the entire set of particles composing a CR (or CR fraction) sample, represented according to the above described models, surface area per unit volume ( $SA_v$ ) was calculated. Consequently, shape and roughness factors to be employed for the computation of surface area by means of equation [1] were derived from the following expressions:

$$w_f = \frac{(SA_v)_E}{(SA_v)_S} \quad w = \frac{(SA_v)_R}{(SA_v)_S} \quad w_r = \frac{w_i}{w_{f,i}} \quad [2]$$

For CR H, values of morphological parameters  $C_f$ ,  $C_s$  and  $\phi_r$  and of surface area  $SA_m$  were calculated as weighted averages of those computed for each single-size fraction. Corrective factor  $\phi$  was thereafter obtained from the inverse of equation [1], and thereafter the roughness factor  $\phi_r$  was computed from equation [2].

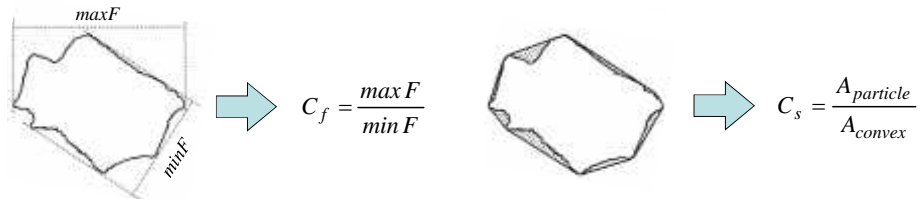


**Figure 1.** Shape and solidity coefficients ( $C_f$  and  $C_s$ ) of CR particles

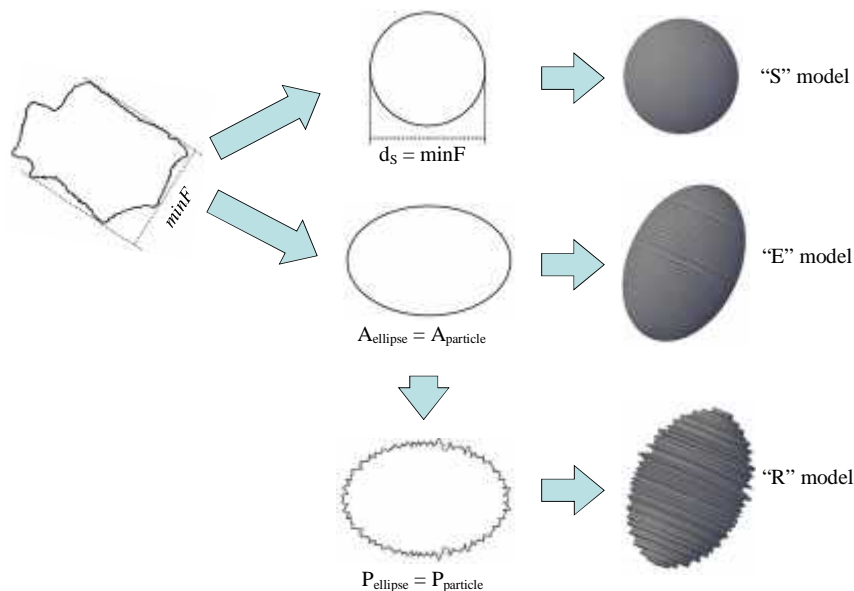


**Figure 2.** Modeling of CR particles for the evaluation of shape and roughness factors ( $W_f$  and  $W_r$ )

### 3.2. Viscosity of asphalt rubber binders

Asphalt rubber binders were subjected to viscosity tests carried out in a wide temperature range (125-190°C) by means of a Brookfield viscometer (DVIII-Ultra). Measurements were performed by employing a SC4-27 spindle at an imposed shear rate equal to  $6.8 \text{ s}^{-1}$  (corresponding to 20 rpm).

## 4. Experimental Results

### 4.1. Characterization of crumb rubber

Size distribution curves of the CRs are shown in Figure 3, while results derived from their analysis and from density tests are listed in Table 2. It can be observed that ambient CRs (A, B and C) are quite similar, with a common value of  $d_{95}$  (i.e. diameter corresponding to 95% passing) equal to 0.71-0.72 mm. The CR product derived from cryogenic processing (G) is clearly finer, with a higher percentage of particles passing the 0.354 mm sieve ( $P_{0.354}$ ) and a value of  $d_{95}$  equal to 0.57 mm. Finally, CR H, obtained by means of the waterjet technology, shows a size distribution which spans in a very wide range, with high values of  $d_{95}$  (equal to 1.02) and of the percentages ( $P_{0.354}$  and  $P_{0.063}$ ) passing the 0.354 and 0.063 mm sieves (respectively equal to 53.8 and 14.3%).

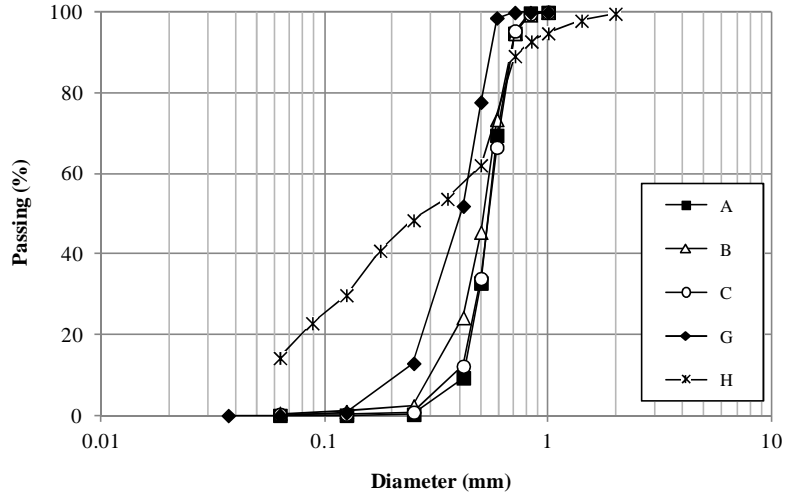


**Figure 3.** Size distribution of CRs

**Table 2.** Size distribution parameters, density and specific gravity of CRs

CR	A	B	C	G	H
$d_{95}$ (mm)	0.71	0.72	0.71	0.57	1.02
$P_{0.354}$ (%)	6.5	17.3	8.6	39.5	53.8
$P_{0.063}$ (%)	0.07	0.58	0.33	0.09	14.3
$\rho$ (g/cm <sup>3</sup> )	1.172	1.181	1.158	1.223	1.189
SG	1.174	1.183	1.160	1.226	1.192

All CRs comply to ASTM standard D6114 which requires the maximum particle diameter to be smaller than 2.36 mm. However, none of them respect gradation criteria which are usually adopted by U.S. Departments of Transportation.

With respect to density, as expected, the highest value was found for the cryogenic CR (G), while the waterjet CR (H) exhibited a value slightly greater than those of ambient CRs (A, B and C). ASTM D6114 acceptance limits for specific gravity ( $1.15 \pm 0.05$ ) were violated only by CR G.

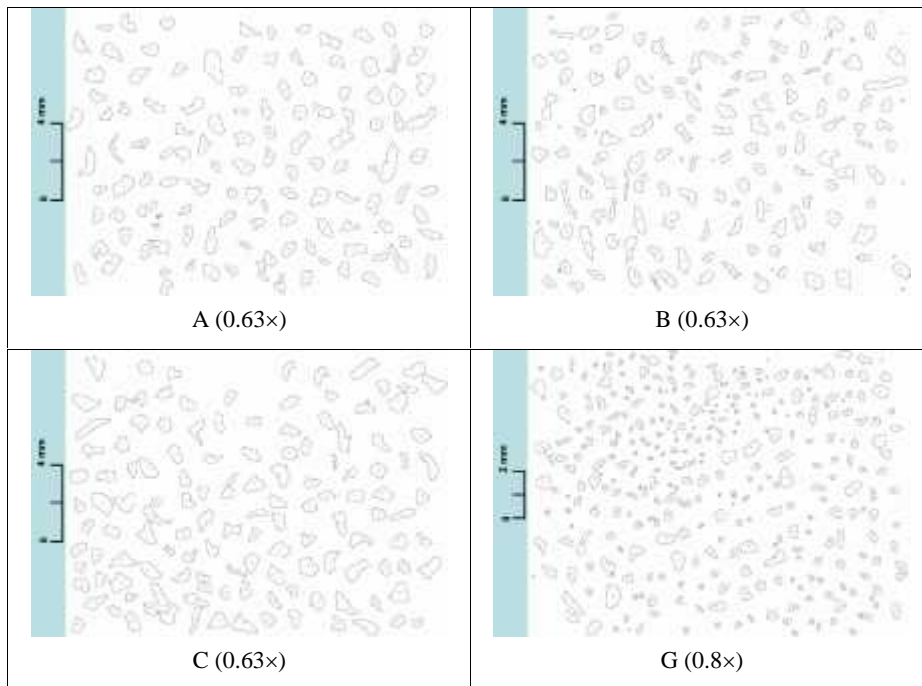
Post-processing images of the CRs and CR H fractions are shown in Figures 4 and 5 respectively, while average values of morphological parameters and calculated surface area are listed in Tables 3 and 4.

**Table 3.** Morphological parameters and surface area of CRs

CR	A	B	C	G	H
$C_f$	1.84	1.89	1.75	1.65	1.65
$C_s$	0.845	0.844	0.849	0.899	0.872
$\phi_f$	1.026	1.066	1.063	1.017	1.034
$\phi_r$	1.236	1.231	1.239	1.148	1.186
$\phi$	1.268	1.313	1.317	1.168	1.226
$SA_m$ (m <sup>2</sup> /g)	0.0126	0.0149	0.0140	0.0160	0.0376
$SA_v$ (m <sup>-1</sup> )	14781	17654	15822	20107	44681

**Table 4.** Morphological parameters and surface area of CR H single-size fractions

Fraction (mesh #s)	12 16	20 24	24 32	32 42	60 80	80 115	115 170	170 250
$C_f$	1.48	1.61	1.67	1.94	1.75	1.55	1.57	1.50
$C_s$	0.894	0.888	0.871	0.856	0.859	0.894	0.864	0.868
$\phi_f$	0.996	1.000	0.987	0.976	0.961	1.081	1.164	1.161
$\phi_r$	1.218	1.207	1.230	1.212	1.154	1.091	1.118	1.103
$\phi$	1.213	1.207	1.214	1.183	1.109	1.180	1.302	1.280
$SA_m$ (m <sup>2</sup> /g)	0.0051	0.0079	0.0101	0.0140	0.0262	0.0394	0.0617	0.0856
$SA_v$ (m <sup>-1</sup> )	6041	9275	12074	16185	31522	46443	73106	104641

**Figure 4.** Post-processing images of CRs

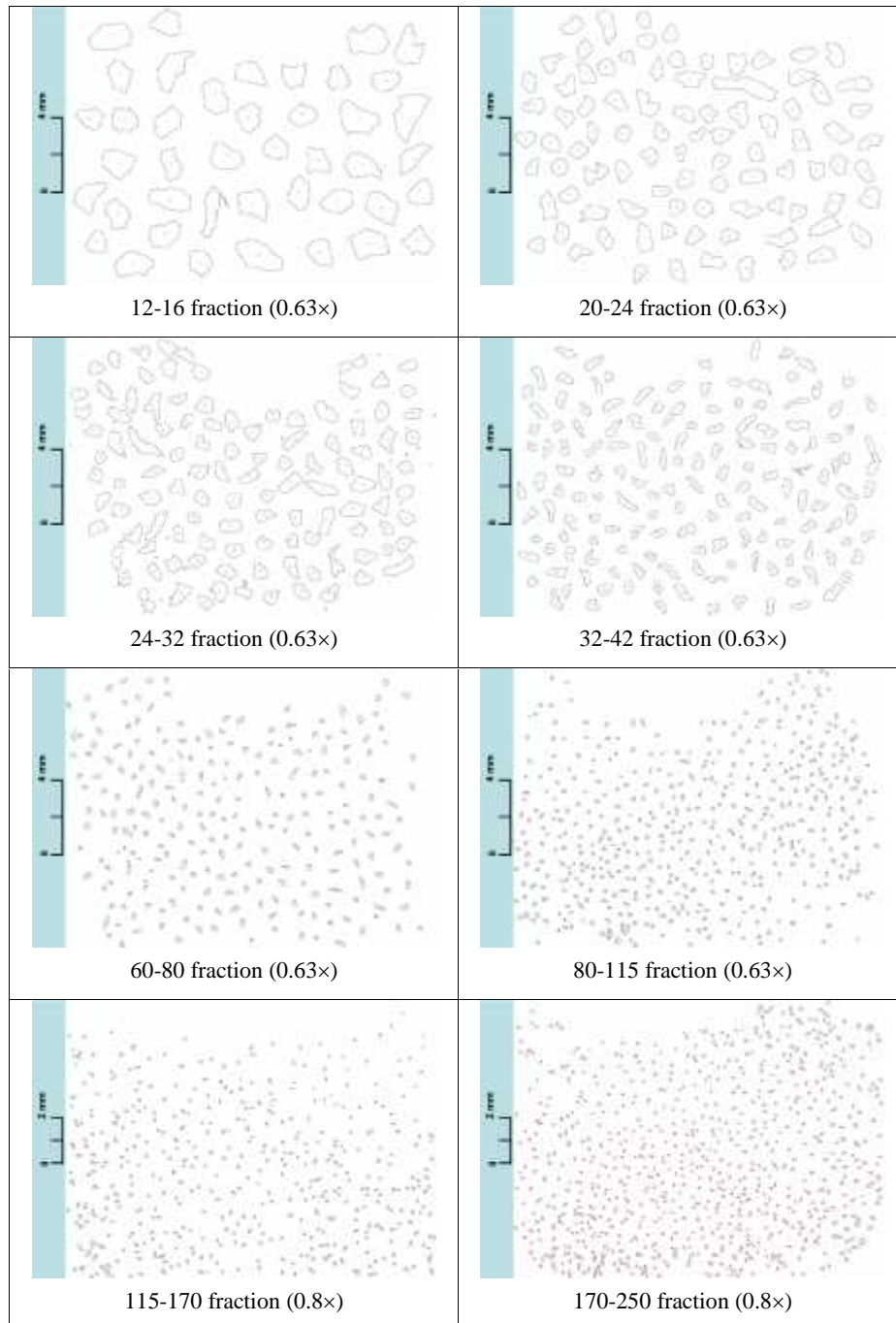


**Figure 5.** Post-processing images of CR H single-size fractions

Assessment of the actual shape and roughness of CR particles stems from the combined analysis of  $C_f$  and  $C_s$  values which are derived from the geometry of their projections on the horizontal plane. While  $C_f$  refers to the degree of elongation,  $C_s$  reveals the presence of surface irregularities which are responsible for a significant increase of the total perimeter. Thus, in general terms, low  $C_f$  values, typical of regularly-shaped particles, may be accompanied, depending upon the specific features of each CR, by either high or low values of  $C_s$ .

Based on these concepts, a shape-roughness mapping plot was built by representing  $C_s$  as a function of  $C_f$  for the five CRs subjected to analysis (Figure 6). Additional data points which are relative to other CRs analyzed with the same technique are included in the graph.

It can be noticed that particles of the cryogenic (G) and waterjet (H) CRs are indeed characterized by a cuboid-type morphology, with a similar low value of  $C_f$  ( $< 1.75$ ). However, as a result of the low-temperature and high-impact production procedure which causes brittle fracture of rubber granules, CR G exhibits a greater solidity associated to a more regular particle surface. Coherently with the milling procedures included in their production processes, ambient CRs show lower values of  $C_s$  (around 0.85). Corresponding values of  $C_f$  are greater than 1.75 and are distributed in a wide interval as a result of specific differences between the various milling processes.

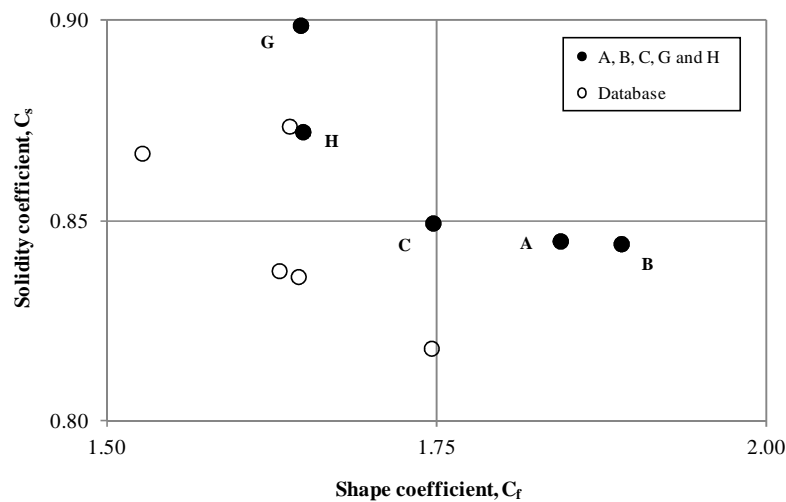


**Figure 6.**  $C_f$ - $C_s$  shape-roughness mapping plot of CRs

By considering the shape coefficients of CR H single-size fractions, it was observed that  $C_f$  and  $C_s$  are a function of particle size as shown in Figures 7 and 8. For the finer fractions (with a nominal diameter smaller than 0.250 mm), as the particles get smaller they tend to be more regularly-shaped (decreasing  $C_f$ ) with a lower presence of surface irregularities (increasing  $C_s$ ). In the case of the coarser fractions ( $d > 0.350$  mm) the opposite trend can be highlighted.

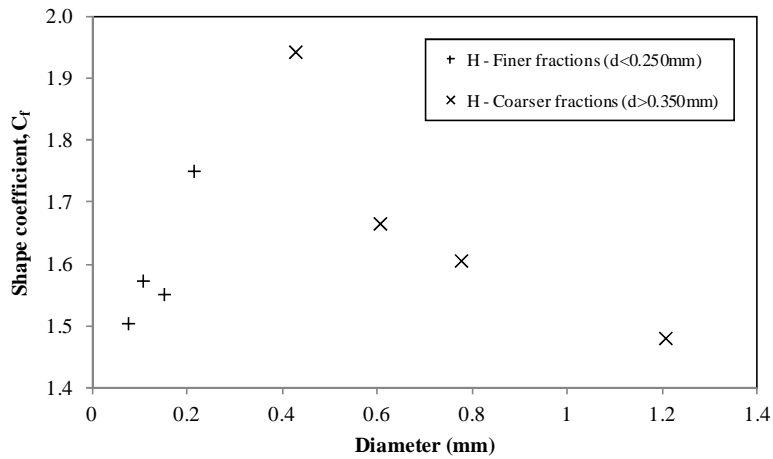


**Figure 7.** Shape coefficient ( $C_f$ ) of CR H single-size fractions

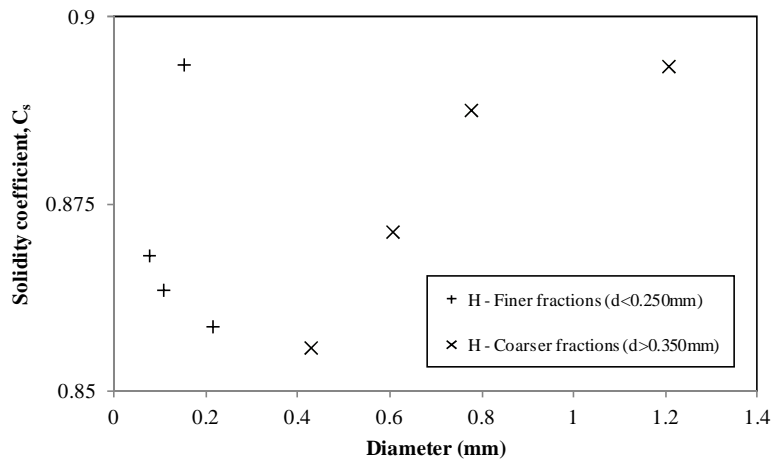


**Figure 8.** Solidity coefficient ( $C_s$ ) of CR H single-size fractions

Shape and roughness factors  $\phi_f$  and  $\phi_r$  defined by the analytical models presented in paragraph 3.1 were found to be sensitive to CR type, thus leading to a composite corrective factor  $\phi$  which is comprised, for the set of considered CRs, between 1.168 and 1.317. While factor  $\phi_f$  is introduced in calculations to compare equivalent ellipsoids to the ideal spheres associated to size distribution analysis (models “E” and “S”), factor  $\phi_r$  is a true indicator of particles roughness, found by comparing the surface area per unit volume of smooth and rough ellipsoids (models “E” and “R”).

As expected, the lowest  $\phi_r$  value was found for the cryogenic CR G (equal to 1.148), while the highest values, all very close to each other, are those of ambient CRs (equal to approximately 1.235). Waterjet CR H exhibits an intermediate  $\phi_r$  value (equal to 1.186).

It is interesting to note that  $C_s$  values derived from the assessment of the individual Feret diameters of the actual particles are coherent with  $\phi_r$  values which stem from the proposed ellipsoidal models (“E” and “R”). This is shown in Figure 9, where data points associated to other CRs characterized with the same methods and models are represented.

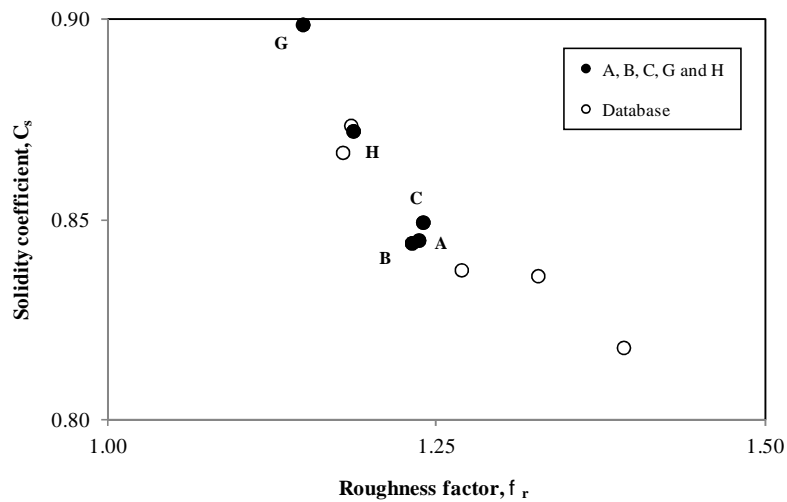


**Figure 9.** Comparison between CR shape factors and coefficients  $w_r$  and  $C_s$

#### 4.2. Characterization of asphalt rubber

Viscosity values measured for the asphalt rubber binders are plotted in Figure 10 as a function of temperature. Experimental data were fitted to a simple power-law model as indicated by the following equation:

$$y(T) = r_T \cdot T^{-s_T} \quad [3]$$

where:  $\eta(T)$  = viscosity (in cP) at temperature T;  
 $\alpha_T$  and  $\beta_T$  = model parameters.

Calculated values of model parameters and coefficients of determination ( $R^2$ ) are reported in Table 5, which also contains the CR percent dosages in the binders expressed both by weight (%CR<sub>w</sub>) and by volume (%CR<sub>v</sub>).

Asphalt rubber prepared with the cryogenic CR (G) exhibits the lowest viscosity values in the entire temperature range, associated to a limited temperature sensitivity (low value of  $\beta_T$ ). Ambient CRs have the highest viscosities and temperature sensitivities. In terms of ranking, CR C, which derives only from truck tyres, is the most effective in stiffening the base bitumen, followed by CR B and CR A. The waterjet CR (H) leads to viscosities which are slightly lower than those of ambient CRs at low temperatures. However, due to its reduced temperature sensitivity ( $\beta_T$  equal to 5.709), the binder approaches the viscosity values of binders containing CRs A and B in the high-temperature range.

All asphalt rubber binders, with the exception of the one containing the cryogenic CR, respect ASTM standard D6114 which requires viscosity at 175°C to be comprised between 1500 and 5000 cP.

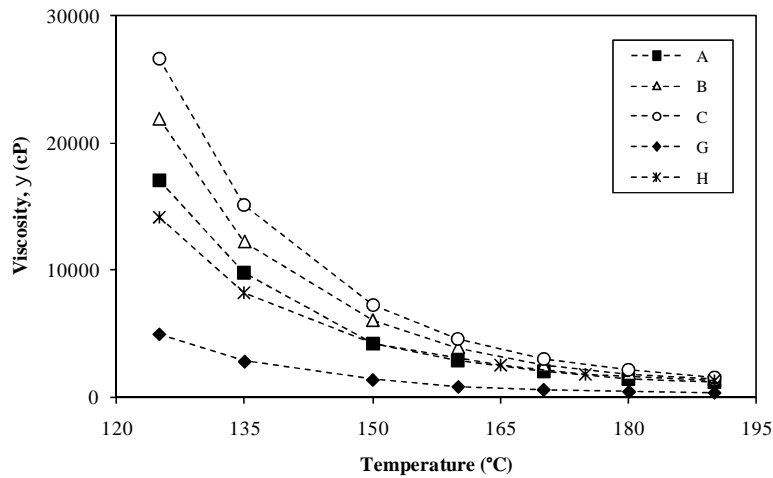


**Figure 10.** Temperature-viscosity curves of the asphalt rubber binders

**Table 5.** CR dosages and viscosity model parameters of the asphalt rubber binders

CR	A	B	C	G	H
%CR <sub>w</sub>	15.0	15.0	15.0	15.0	15.0
%CR <sub>v</sub>	15.1	15.0	15.3	14.5	14.9
$\alpha_T$	6.39E+17	1.70E+18	3.91E+18	3.63E+16	1.22E+16
$\beta_T$	6.491	6.636	6.765	6.153	5.709
$R^2$	0.9920	0.9972	0.9981	0.9889	0.9931

## 5. Modeling

In order to investigate the relationship between flow behaviour of asphalt rubber binders and morphological and physical characteristics of CR, the experimental data synthesized in paragraphs 4.1 and 4.2 were analyzed jointly and then employed for the identification of a viscosity prediction model. Given the limited set of experimental data available, emphasis of modeling was not placed on the minimization of the total prediction error, but rather on its conceptual implications. For the same reasons, the maximum number of independent variables were limited to four to reduce the possibility of selecting random regressor combinations.

It was assumed that viscosity variations have to be explained by taking into account the variations of temperature and of the parameters which are combined in equation [1] for the calculation of surface area. Therefore, the additional three independent variables related to CR characteristics and selected for the formulation of the model were the following:

- density ( $\rho$ ), which is related to the composition and surface porosity of the particles and allows to take into account the effective volume occupied by different CRs with the same dosage by weight;
- corrective factor ( $\phi$ ) derived from the analytical three-dimensional modeling of surface area, which provides a quantitative measure of particle shape and roughness;
- surface area per unit volume calculated by considering spherical particles with the effective size distribution of CR ( $6 \cdot \sum_i f_i / d_{m,i}$ ).

Based on the discussion provided above, the following model was identified and thereafter subjected to statistical evaluation:

$$y = 10^{a_1} \cdot T^{-a_2} \cdot \dots^{-a_3} \cdot W^{a_4} \cdot \left( 6 \cdot \sum_i \frac{f_i}{d_{m,i}} \right)^{a_5} \quad [4]$$

where:  $\eta$  = viscosity (in cP) of asphalt rubber binder;  
 $T$  = temperature (in °C);  
 $\rho$  = density of CR (in g/cm<sup>3</sup>);  
 $\phi$  = corrective factor of surface area (non dimensional);  
 $6 \cdot \sum_i f_i / d_{m,i}$  = surface area per unit volume of spheres with the size distribution of CR (in m<sup>-1</sup>);  
 $a_1, a_2, a_3, a_4$  and  $a_5$  = model parameters.

Signs attributed to the exponents of the independent variables included in equation [4] were fixed by considering the physical phenomena which are believed to explain viscosity variations. In particular, coherently with findings of previous studies (West *et al.*, 1998), it was assumed that increasing temperature and density values lead to a viscosity reduction (negative exponents). The positive exponent of corrective factor  $\phi$  is coherent with its definition, since increasing deviations of the modeled particles from the ideal smooth spheres certainly cause a viscosity increase.

Finally, no assumption was made on the sign of the last exponent since it has been well documented that viscosity can either increase or decrease as a function of surface area depending upon whether particle size or surface interaction effects become predominant in the CR-bitumen system (Shen *et al.*, 2009a,b).

Values of model parameters ( $a_i$ ) obtained by fitting experimental data to the logarithmic expression of equation [4] by means of linear regression are shown in Table 6, which also contains related standard errors ( $se_i$ ). Coefficients of determination  $R^2$  and  $\bar{R}^2$  (adjusted) were found to be respectively equal to 0.993 and 0.991. By calculating t-statistics of model parameters and by assuming a critical alpha level equal to 0.05, it was verified that all the variables used in the model are statistically significant in predicting viscosity.

**Table 6.** Parameters and standard errors of the viscosity prediction model

	i = 1	i = 2	i = 3	i = 4	i = 5
Model parameter $a_i$	15.65	6.36	12.62	0.443	8.93
Standard error $se_i$	0.45	0.12	2.18	0.05	0.94

Figure 11 shows the relationship between measured and predicted viscosity values, with data points that are well grouped around the equality line. Percent errors calculated with respect to true measured viscosities are represented in Figure 12, where they are compared to those deriving from the use of temperature-viscosity power-law models applied to each CR type.

It can be observed that the model leads to an underestimate of viscosity in the low and high temperature range, while at intermediate temperatures it overestimates true (measured) values. Percent errors are mostly comprised within  $\pm 15\%$ , with higher absolute values generally occurring at extreme temperatures.

It should also be pointed out that errors associated to the model are comparable to those of the individual power-law equations. This clearly indicates that the main source of error relies in the choice of the type of temperature dependency and not in the selection of the prediction variables or in the overall structure of the model.

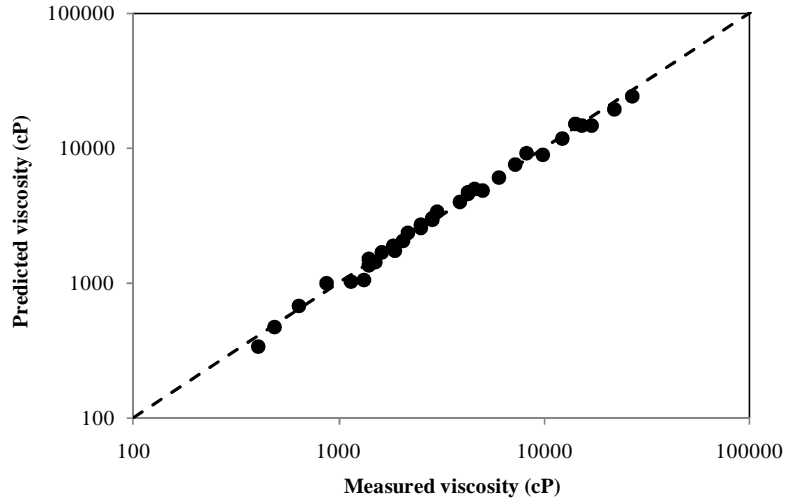


Figure 11. Comparison between measured and predicted viscosity values

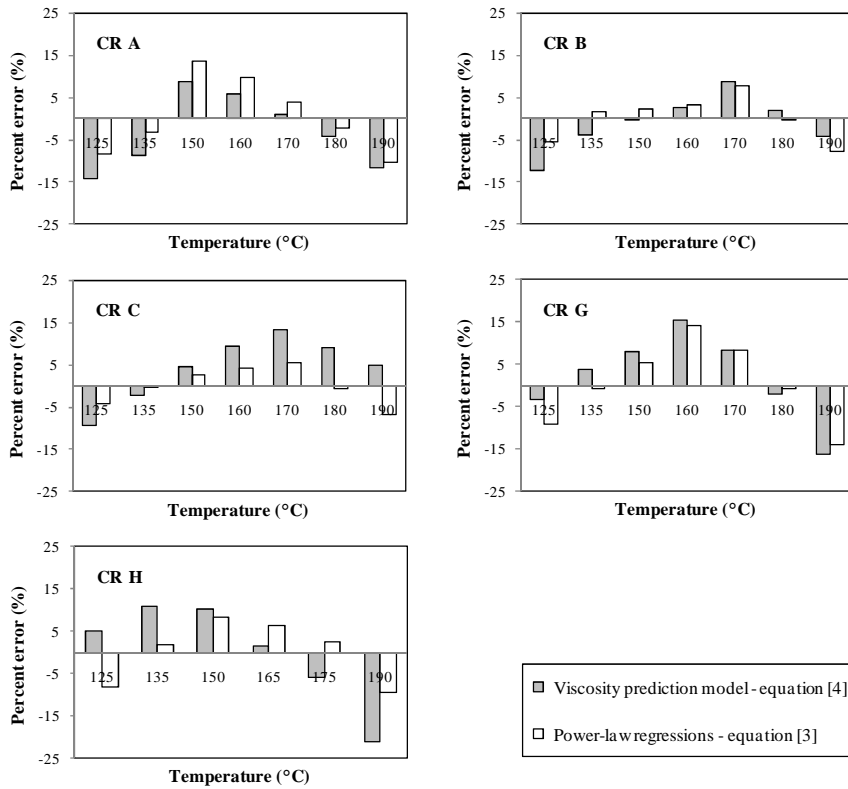


Figure 12. Percent errors of prediction model and power-law regressions

## 5. Conclusions

Experimental results obtained in the investigation described in this paper contribute to the general understanding of the mechanisms of interaction between crumb rubber (CR) and bitumen in asphalt rubber binders. Specific conclusions can be drawn with respect to the innovative procedures and models proposed for the evaluation of CR morphology, to the comparative evaluation of different CR types and of their corresponding asphalt rubber binders, and to the use of a prediction model for estimating binder viscosity.

Procedures and models developed for the assessment of CR morphology are based on the combined use of microscopic observations, image analysis algorithms and three-dimensional analytical models of CR particles. Validity of such an approach is confirmed by the coherency of the results with the peculiarities of CR production processes and with general information available in literature. It should be also mentioned that the tools required for characterization are simple and affordable and therefore easily accessible on a widespread basis to the research and engineering community.

CRs subjected to evaluation included products deriving from ambient, cryogenic and high pressure waterjet size-reduction processes. By making use of the abovementioned characterization techniques, it was confirmed that cryogenic products are composed of particles which are definitely smoother and more regularly shaped than those of ambient CRs. Nevertheless, surface area was found to be higher for the cryogenic CR due to a finer size distribution. Viscosity of the binders containing ambient CRs was definitely higher than that of asphalt rubber prepared with the same dosage of cryogenic CR. Moreover, the highest viscosity values were measured for the binder prepared with the ambient CR derived exclusively from truck tyres, which contains a higher percentage of natural rubber.

Due to the novelty of the production process, conclusions regarding the waterjet CR are of great interest in the light of its possible use in asphalt rubber. It was found that its morphological properties are intermediate between ambient and cryogenic CRs, while flow properties of the corresponding asphalt rubber binder are comparable, at high temperatures, to those of binders containing ambient CRs.

Based on the available experimental data, a prediction model was developed for binder viscosity in order to highlight its dependency upon the physical and morphological properties of CR. Even though the database was quite limited, the model proved to be statistically sound and coherent with interaction phenomena which occur within asphalt rubber binders. Despite these encouraging results, refinements are certainly needed to validate the model with a wider set of materials and to take into account additional important factors such as bitumen type, CR composition and CR dosage.

## 6. Bibliography

- ASTM D6114, American Society of Testing and Materials, “D 6114 Standard specification for asphalt rubber binder”, *Annual Book of ASTM Standards, Vol. 4.03*, ASTM, 2004.
- Hicks, R.G., *Asphalt rubber design and construction guidelines. Volume 1 - Design guidelines*, Northern California Rubberized Asphalt Concrete Technology Center (NCRACTC) - California Integrated Waste Management Board (CIWMB), 2002.
- Lee, S., Akisetty, C. K., Amirkhanian, S., “The effect of crumb rubber modifier (CRM) on the performance properties of rubberized binders in HMA pavements”, *Construction and Building Materials*, 22 (2008), pp. 1368–1376.
- Putman, B.J., Amirkhanian S., “Crumb rubber modification of binders: interaction and particle effects”, *Asphalt Rubber 2006 Conference*, Palm Springs, CA, 2006.
- Santagata, E., Zanetti, M.C., *Technologies for the use in road pavements of crumb rubber products deriving from end-of-life-tyres*, Technical Report, ECOPNEUS, 2012.
- Shen, J., Amirkhanian, S., Xiao, F., Tang B., “Surface area of crumb rubber modifier and its influence on high-temperature viscosity of CRM binders”, *International Journal of Pavement Engineering*, 10 (5) (2009), pp. 375–381.
- Shen, J., Amirkhanian, S., Xiao, F., Tang, B., “Influence of surface area and size of crumb rubber on high temperature properties of crumb rubber modified binders”, *Construction and Building Materials*, 23 (2009), pp. 1304–1310.
- Shen, J., Amirkhanian, S., “The influence of crumb rubber modifier (CRM) microstructures on the high temperature properties of CRM binders”, *International Journal of Pavement Engineering*, 6 (4) (2005), pp. 265–271.
- State of California Department of Transportation, *Use of scrap tire rubber. State of the technology and best practices*, 2005.
- Thodesen, C., Shatanawi, K., Amirkhanian, S., “Effect of crumb rubber characteristics on crumb rubber modified (CRM) binder viscosity”, *Construction and Building Materials*, 23 (2009), pp. 295–303.
- West, R.C., Page, G.C., Veilleux, J., “Effect of tyre rubber grinding method on asphalt-rubber binder characteristics”, *Proceedings of the TRB Annual Meeting*, 1998.
- Zanetti, M.C., Fiore, S., Ruffino, B., Santagata, E., “End of life tyres: crumb rubber physical and chemical characterization for reuse in paving applications”, *Thirteenth International Waste Management and Landfill Symposium*, S. Margherita di Pula, Italy, 2011.

## Acknowledgements

The investigation described in this paper was carried out as part of LIFE+ project entitled “Development and Implementation of Innovative and Sustainable Technologies for the Use of Scrap Tyre Rubber in Road Pavements (TYREC4LIFE)”. In such a context, the support of ECOPNEUS s.c.p.a. is gratefully acknowledged.